Effect of anomalous electron heating on the transpolar potential in the LFM global MHD model

V. G. Merkin,[1] G. Milikh,[2] K. Papadopoulos,[2] J. Lyon,[3] Y. S. Dimant,[1] A. S. Sharma,[2] C. Goodrich,[1] and M. Wiltberger[4]

Received 22 April 2005; revised 15 July 2005; accepted 6 October 2005; published 16 November 2005.

[1] The tendency of global MHD models to overestimate the transpolar potential in simulations of strong geomagnetic storms and evidence of an adverse feedback of the ionospheric conductance on the potential suggest that these models lack important physics leading to the conductance enhancement. Farley-Buneman instability in the auroral ionosphere provides this lacking physics. This instability is believed to cause strong anomalous electron heating which affects the ionospheric conductivity. We use an earlier developed model of anomalous electron heating to estimate the ionospheric conductance disturbance as a function of the local electric field. This result is used to modify the ionospheric conductance in the LFM model to study its effect on the simulated transpolar potential. An idealized and a real-case simulations are accomplished. In both cases a considerable drop in the simulated transpolar potential is found. The latter is in a good agreement with AMIE model and DMSP data. **Citation:** Merkin, V. G., G. Milikh, K. Papadopoulos, J. Lyon, Y. S. Dimant, A. S. Sharma, C. Goodrich, and M. Wiltberger (2005), Effect of anomalous electron heating on the transpolar potential in the LFM global MHD model, *Geophys. Res. Lett.*, *32*, L22101, doi:10.1029/2005GL023315.

1. Introduction

[2] The behavior of the transpolar potential is an important signature of magnetic storms. Observations show that while for low or moderate solar wind drivers (IEF < 5 mV/m) the transpolar potential varies linearly with the convective solar wind electric field it exhibits saturation at higher electric field values. Global MHD models have been successful in modeling the behavior of the transpolar potential for low or moderate drivers as well as predicting saturation for stronger drivers [*Siscoe et al.*, 2002; *Merkin et al.*, 2005]. However, they usually predict a significantly higher value of the saturated potential than observed. In this letter we demonstrate that incorporating physics due to microinstability driven turbulent heating in the ionospheric conductance algorithms leads to simulated transpolar potentials consistent with observations.

[1]Center for Space Physics, Boston University, Boston, Massachusetts, USA.
[2]Department of Astronomy, University of Maryland, College Park, College Park, Maryland, USA.
[3]Department of Physics and Astronomy, Dartmouth College, Hanover, New Hampshire, USA.
[4]High Altitude Observatory, National Center for Atmospheric Research, Boulder, Colorado, USA.

Copyright 2005 by the American Geophysical Union.
0094-8276/05/2005GL023315$05.00

[3] Global MHD simulations [*Fedder and Lyon*, 1987; *Raeder et al.*, 2001; *Ridley et al.*, 2004; *Merkin et al.*, 2005], as well as observations [*Ober et al.*, 2003] indicate that the transpolar potential is affected by the ionospheric conductance. In the Hill/Siscoe model [*Siscoe et al.*, 2002] saturation of the transpolar potential occurs due to the feedback of the conductance-dependent field-aligned currents on the day side reconnection potential. *Merkin et al.* [2005] described another mechanism of the ionospheric conductance feedback on the day side reconnection potential and suggested that saturation can occur due to increase in the conductance during disturbed conditions.

[4] In global MHD codes, the ionospheric conductance is specified by algorithms that involve only EUV ionization and contributions due to auroral particle precipitation [e.g., *Fedder et al.* 1995]. However, numerous radar observations indicate that the electron temperature in the high latitude electrojet increases dramatically during magnetic storms [*Schlegel and St.-Maurice*, 1981; *Foster and Erickson*, 2000]. Analysis and observations attribute the elevated electron temperature to turbulent heating caused by the Farley-Buneman instability [*Farley*, 1963; *Ossakow et al.*, 1975]. The instability develops in the altitude region between 90–120 km, where the electrons are magnetized while the ions are not, when the electron drift velocity exceeds the sound speed. This corresponds to a threshold ionospheric electric field of approximately 20 mV/m. For electric fields exceeding this threshold, the instability leads to turbulent (anomalous) electron heating. The higher electron temperature has a strong overall effect on the height integrated conductivities through the electron-ion recombination rate.

[5] In this paper, the effect of the anomalous electron heating on the transpolar potential is studied using the Lyon-Fedder-Mobarry (LFM) global MHD model [*Lyon et al.*, 2004]. A new algorithm was developed and incorporated in the ionospheric part of the LFM model to introduce contribution of the anomalous electron heating to the ionospheric conductance. LFM simulations for idealized solar wind and ionosphere parameters, as well as for a 12 hour period during the Halloween Storm of 29–30 October 2003, are discussed next.

2. Effect of Anomalous Electron Heating on the Ionospheric Conductances

[6] Models of anomalous electron heating by the Farley-Buneman instability have been developed and tested against incoherent scatter radar data during the last two decades [*Providakes et al.*, 1988; *St.-Maurice et al.*, 1990]. The algorithm incorporated into the LFM model is derived from

the recent theoretical analysis by *Dimant and Milikh* [2003], which is based on nonlinearly saturated turbulence coupled to numerical solutions of the electron and ion energy balance equations. The results of this model were checked against incoherent scatter radar observations [*Foster and Erickson*, 2000].

[7] At the altitudes of interest (90–120 km) the ion contribution to the Pedersen conductivity dominates the electron contribution and the total Pedersen conductance can be represented as

$$\Sigma_P \simeq \int \frac{e^2 n \, dz}{g_{NO^+} m_{NO^+} \nu_{NO^+} + g_{O_2^+} m_{O_2^+} \nu_{O_2^+}} \tag{1}$$

where $n(z)$ is the electron density, z is the altitude, g_{NO^+} and $g_{O_2^+}$ are mixing ratios of the two dominant ion species NO^+ and O_2^+, m_{NO^+} and $m_{O_2^+}$ are masses of these ions, while ν_{NO^+} and $\nu_{O_2^+}$ are their collision frequencies with the neutral particles. The Hall conductance disturbance is also taken into account in our calculation, although its effect on the transpolar potential is insignificant, since the Hall current closure occurs along the trajectory perpendicular to the electric field. The code has been run with and without the Hall conductance disturbance, and this assertion has been verified within ~5–10% accuracy.

[8] The ionospheric conductivities can be affected by anomalous electron heating only through the changes in plasma density [*Schlegel and St.-Maurice*, 1981]. The increase in the plasma density n is the result of the decrease in the electron-ion recombination rate α with the electron temperature. Under stationary conditions, it is given by $n = n_0\sqrt{\alpha_0/\alpha}$ [*Gurevich*, 1978], where according to *Huba et al.* [2000],

$$\alpha(\mathrm{cm}^3/\mathrm{s}) = 4.2 \times 10^{-7}(T_0/T_e)^{0.85} g_{NO^+} + 1.6 \times 10^{-7}(T_0/T_e)^{0.55} g_{O_2^+} \tag{2}$$

and T_0, n_0, and α_0 are the unperturbed electron temperature, density, and recombination rate: $\alpha_0 = \alpha(T_e = T_0)$, $n_0 = n(T_e = T_0)$.

[9] In developing the conductance algorithm the ambient electron density and the mixing ratios of NO^+ and O_2^+ ions were taken from the International Reference Ionosphere (web address: http://nssdc.gsfc.nasa.gov/space/model/models/iri_html). The electron temperature as a function of altitude and of the convective electric field was taken from *Milikh and Dimant* [2003], Figure 8. The ion collision frequencies were found by using momentum transfer collision frequencies for ion-neutral interactions [*Schunk and Nagy*, 2000] while the neutral density and temperature were taken from MSIS-E-90 Atmosphere Model (web address: http://nssdc.gsfc.nasa.gov/space/model/models/msis.html). The ambient and perturbed conductances were computed from equations (1)–(2) by using the previously mentioned model data along with the $T_e(z, E_C)$ dependence, where E_C is the local convective electric field, from *Milikh and Dimant* [2003].

[10] Figure 1 shows the calculated ratio of the disturbed to quiet Pedersen (a) and Hall (b) conductances as a function of E_C for the daytime (dashed) and nighttime (dash-dot) conditions, corresponding to the date of the real event simulation described below (30 Oct 2003) at 65°N. The solid line is the square root dependence, $\Sigma_{P,H}/\Sigma^0_{P,H} = \sqrt{E_C/E_{thr}}$, where E_{thr} = 20 mV/m is the instability threshold electric field.

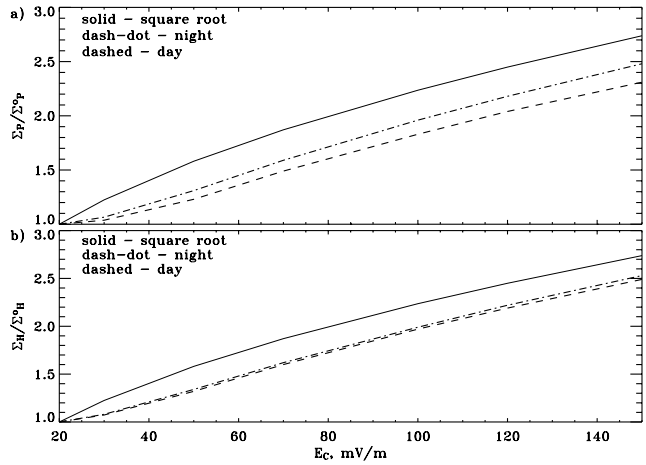

Figure 1. (a) Pedersen and (b) Hall conductance disturbances as functions of the convective electric field.

[11] Figure 1 demonstrates that the ratio $\Sigma_{P,H}/\Sigma^0_{P,H}$ is a nonlinear function of the convective electric field, and that $\Sigma_{P,H}$ can be disturbed up to as much as 2.5 times their unperturbed value, when the electric field E_C approaches 150 mV/m. It is worth noting, that the ambient Hall conductivity peaks at about 110 km for the nighttime as well as daytime. Thus, the relative increase in Σ_H is almost the same at the day and nighttime. For the ambient Pedersen conductivity, however, the nighttime peak is still located at 110 km, while the daytime peak is shifted to higher altitudes 120–130 km. Thus, the anomalous electron heating, which is effective at 100–120 km, has a smaller effect on Σ_P at the daytime compared to the nighttime.

3. Anomalous Electron Heating in the LFM Simulations

[12] One expects that perturbations of the ionospheric conductance as strong as those shown in Figure 1 will affect the ionospheric solution of a global MHD model. In the LFM model the ionospheric simulation solves the height-integrated Poisson equation:

$$\nabla_\perp(\bar{\Sigma}\nabla_\perp\Phi) = j_\parallel, \tag{3}$$

where $\bar{\Sigma}$ is the conductance tensor, Φ is the electrostatic potential, and $j_\parallel$ is the field aligned current (see *Lyon et al.* [2004] and references therein for details). The conductance tensor contains the height-integrated Hall and Pedersen conductivities that can be either set to a constant value uniformly over the entire polar cap or calculated from an empirical model including EUV ionization and auroral precipitation [*Fedder et al.*, 1995].

[13] In this section we test the response of the LFM model to the changes in the ionospheric conductance shown in Figure 1. This is accomplished by incorporating in the LFM an algorithm that compares at every time step the local electric field computed from the solution of Poisson equation (3) with the threshold value for the instability and if larger adjusts the conductances to the values given by Figure 1. A drawback of this approach is that both the quiet and disturbed ionospheric conductances used to obtain the profiles in Figure 1 are calculated using the

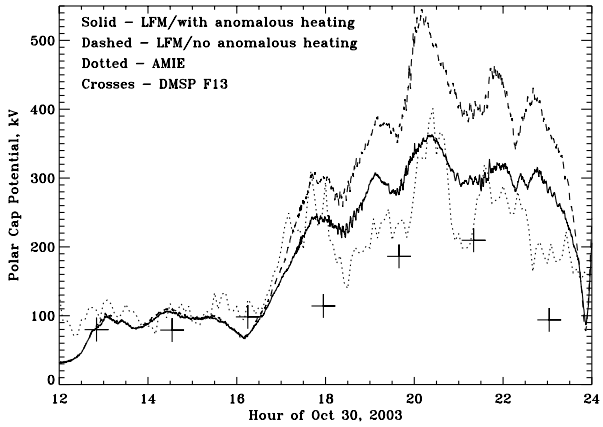

Figure 2. Northern Hemisphere transpolar potential calculated using the indicated models and the DMSP F13 passes.

averaged ionosphere and atmosphere models mentioned in section 2, which do not include an auroral oval. Then the LFM conductance is modified based on the value of the disturbance in Figure 1. A self-consistent approach to the problem at hand would be to incorporate the anomalous electron heating rate in an ionosphere-thermosphere model (ITM) energy balance equations, and then use the ITM conductances to drive the ionospheric simulation of the global MHD model. Such a study is currently in progress, while this paper shows a "proof of principle", namely that the anomalous electron heating may be very important globally for the evolution of the entire magnetosphere-ionosphere system.

[14] We first run simulations using an idealized solar wind and ionospheric model with the solar wind propagating strictly earthward with 400 km/sec speed, number density 30 cm^{-3}, and southward IMF (B_z = −40 nT) that corresponds to a strong driver (IEF of 16 mV/m). Two simulations were performed: One with 10 S uniform Pedersen conductance and no anomalous heating and one with the anomalous heating algorithm, where $\Sigma_P(E_C)$ dependence is modeled through the square root function shown in Figure 1, and the same background conductance. In both cases the solution converged to a steady state within 1–2 hours following the southward turning of the IMF. However, the steady state polar cap potential was found to equal 221 kV in the presence of anomalous heating as opposed to 352 kV without it.

[15] Next we simulated a real event that occurred on October 29–30, 2003 (Halloween Storm) using solar wind data from the ACE SWEPAM instrument [*Skoug et al.*, 2004]. In this case the background ionospheric conductance was calculated using the empirical model [*Fedder et al.*, 1995] and the anomalous heating was modeled using the day and night profiles shown in Figure 1. To analyze the effect of anomalous electron heating on the LFM transpolar potential we choose a period from ∼1200 UT to ∼2400 UT on October 30. This is one of the periods during the indicated 2-day interval when extremely high solar wind speeds were observed. Despite moderate magnitude of the southward B_Z the IEF at times exceeded 30 mV/m resulting in large convective ionospheric electric fields expected to cause strong anomalous electron heating.

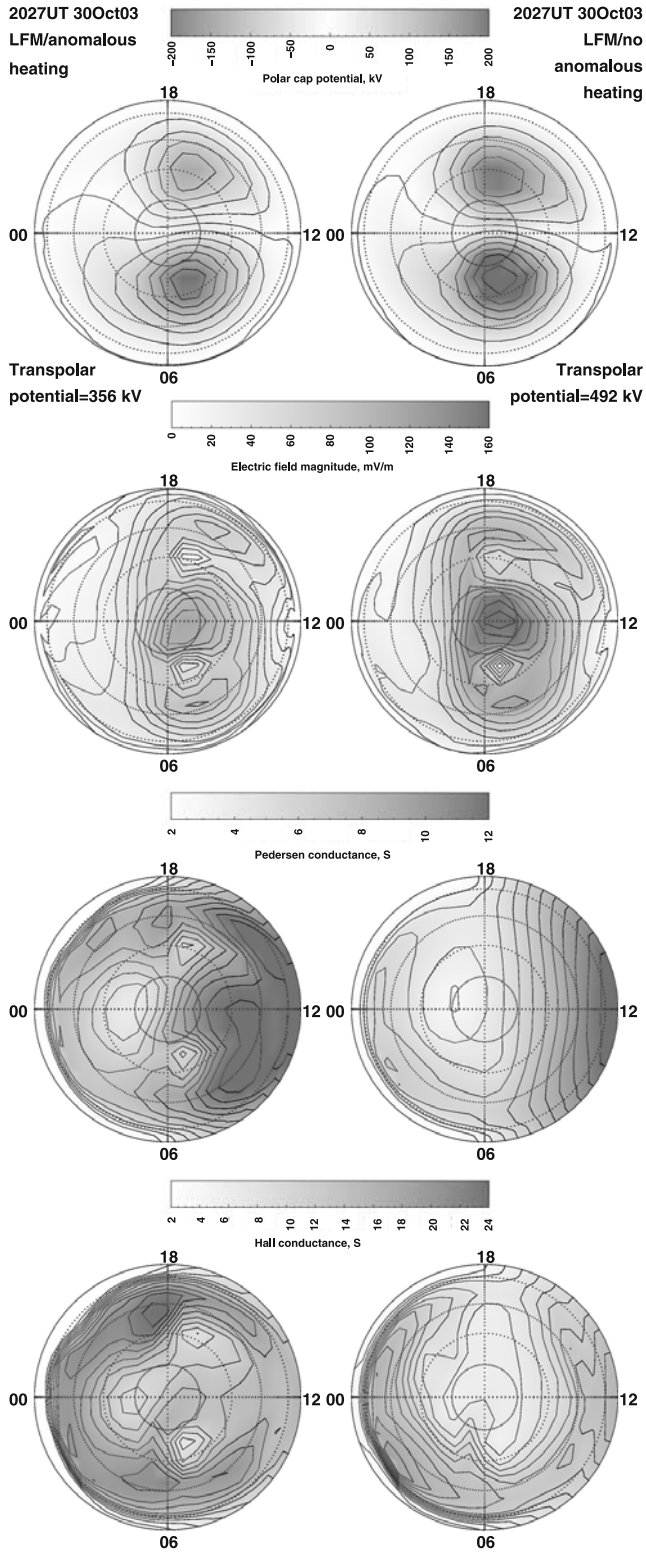

Figure 3. Comparison of the simulated ionospheric quantities in the Northern Hemisphere. Note, the potential in the first panel is negative in the dusk and positive in the dawn sector convection cell. See color version of this figure in the HTML.

[16] Figure 2 shows the comparison of the LFM Northern Hemisphere transpolar potential calculated using the conventional LFM ionospheric model (dashed line) and that model with the contribution of anomalous electron heating to the ionospheric conductance (solid line). The difference is quite remarkable. It is ~135 kV around 2027UT (about 10–20 min after the peak) which constitutes 30% of the unmodified value. For comparison, the dotted line in the figure shows the AMIE [*Richmond and Kamide*, 1988] transpolar potential as well as the potential recovered from the DMSP F13 polar passes (crosses). In general, the LFM transpolar potential that incorporates the physics of the anomalous electron heating is in much better agreement with the AMIE data than the conventional one. The DMSP values are generally lower than both AMIE and LFM but the F13 satellite does not necessarily pass through the extreme values of the potential and thus underestimates it.

[17] Figure 3 compares ionospheric quantities in the Northern Hemisphere for the conventional and modified LFM models. The plots correspond to 2027UT. The top panel shows that while the magnitude of the ionospheric potential is smaller in the modified LFM model, the geometry of the pattern is preserved. This indicates that the changes in the ionosphere do not affect significantly the simulated magnetosphere. This is confirmed by the magnetospheric solution (not shown here). This is explained by the fact that under such intense driving it is not very difficult for the solar wind flow to accommodate an additional 130 kV potential drop. Indeed, this drop corresponds to only 0.7 R_e increase in the geoeffective distance in the solar wind, for 30 mV/m IEF.

[18] The 2nd, 3rd, and 4th panels in Figure 3 show the changes in the electric field and the Pedersen and Hall conductances, respectively. As expected, the conductances are enhanced in the regions of the high electric field, while the latter is reduced due to the enhanced conductance. This indicates a drawback in the current approach: When the conductance depends on the value of the electric field, equation (3) becomes nonlinear requiring an iterative solution. Possible nonlinear feedback effects are currently under study.

4. Summary

[19] In summary, we have modified the ionospheric part of the LFM global MHD model to include anomalous electron heating in the calculation of the ionospheric conductance. The dependence of the conductance on the local convective electric field is estimated using the model of the saturated Farley-Buneman instability [*Dimant and Milikh*, 2003]. Incorporating the physics of the anomalous electron heating results in significant drop of the simulated transpolar potential. This result can, at least partly, explain the tendency of strongly driven global MHD models to overestimate the transpolar potential. Further, the adverse effect of the enhanced ionospheric conductance on the transpolar potential can account for its saturation. The plausibility of such an explanation is supported by the threshold-like dependence of the conductance disturbance upon the local ionospheric and solar wind electric field.

[20] **Acknowledgments.** We appreciate greatly assistance of Gang Lu and Mark Hairston in obtaining the AMIE and DMSP transpolar potentials, respectively. We thank the ACE SWEPAM and Geotail PWI teams for the solar wind data. We thank NCAR Scientific Computing Division and the Boston University Scientific Computing and Visualization Group for the computational resources. This research was supported by NSF grant ATM-0334256 and NASA grants NAG513452 and NAG510882.

References

Dimant, Y. S., and G. M. Milikh (2003), Model of anomalous electron heating in the E region: 1. Basic theory, *J. Geophys. Res.*, *108*(A9), 1350, doi:10.1029/2002JA009524.

Farley, D. T. (1963), A plasma instability resulting in field aligned irregularities in the ionosphere, *J. Geophys. Res.*, *68*, 6083–6097.

Fedder, J. A., and J. G. Lyon (1987), The solar wind-magnetosphere-ionosphere current-voltage relationship, *Geophys. Res. Lett.*, *14*, 880–883.

Fedder, J. A., S. P. Slinker, J. G. Lyon, and R. D. Elphinstone (1995), Global numerical simulation of the growth phase and the expansion onset for substorm observed by Viking, *J. Geophys. Res.*, *100*, 19,083–19,093.

Foster, J. C., and P. J. Erickson (2000), Simultaneous observations of E-region coherent backscatter and electric field amplitude at F-region heights with the Millstone Hill ULF radar, *Geophys. Res. Lett.*, *27*, 3177–3180.

Gurevich, A. V. (1978), *Nonlinear Phenomena in the Ionosphere*, pp. 96–99, Springer, New York.

Huba, J. D., G. Joyce, and J. A. Fedder (2000), Sami2 is Another Model of the Ionosphere (SAMI2): A new low-latitude ionosphere model, *J. Geophys. Res.*, *105*, 23,035–23,053.

Lyon, J. G., J. A. Fedder, and C. M. Mobarry (2004), The Lyon-Fedder-Mobarry (LFM) global MHD magnetospheric simulation code, *J. Atmos. Sol. Terr. Phys.*, *66*, 1333–1350, doi:10.1016/j.jastp.2004.03.020.

Merkin, V. G., A. S. Sharma, K. Papadopoulos, G. Milikh, J. Lyon, and C. Goodrich (2005), Global MHD simulations of strongly driven magnetosphere: Modeling of the transpolar potential saturation, *J. Geophys. Res.*, *110*, A09203, doi:10.1029/2004JA010993.

Milikh, G. M., and Y. S. Dimant (2003), Model of anomalous electron heating in the E region: 2. Detailed numerical modeling, *J. Geophys. Res.*, *108*(A9), 1351, doi:10.1029/2002JA009527.

Ober, D. M., N. C. Maynard, and W. J. Burke (2003), Testing the Hill model of transpolar potential saturation, *J. Geophys. Res.*, *108*(A12), 1467, doi:10.1029/2003JA010154.

Ossakow, S. L., K. Papadopoulos, J. Orens, and T. Coffey (1975), Parallel propagation effects on the type 1 electrojet instability, *J. Geophys. Res.*, *80*, 141–148.

Providakes, J., D. T. Farley, B. G. Fejer, J. Sahr, W. E. Swartz, I. Haggstrom, A. Hedberg, and J. A. Nordling (1988), Observations of auroral E-region plasma waves and electron heating with ESICAT and VHF radar interferometer, *J. Atmos. Terr. Phys.*, *50*, 339–356.

Raeder, J., et al. (2001), Global simulation of the Geospace Environment Modeling substorm challenge event, *J. Geophys. Res.*, *106*, 381–395.

Richmond, A. D., and Y. Kamide (1988), Mapping electrodynamic features of the high-latitude ionosphere from localized observations: Technique, *J. Geophys. Res.*, *93*, 5741.

Ridley, A. J., T. I. Gombosi, and D. L. De Zeeuw (2004), Ionospheric control of the magnetosphere: conductance, *Ann. Geophys.*, *22*, 567–584.

Schlegel, K., and J. P. St.-Maurice (1981), Anomalous heating of the polar E region by unstable plasma waves: 1. Observations, *J. Geophys. Res.*, *86*, 1447–1452.

Schunk, R. W., and A. F. Nagy (2000), *Ionospheres Physics, Plasma Physics, and Chemistry*, Cambridge Univ. Press, New York.

Siscoe, G. L., G. M. Erickson, B. U. Ö. Sonnerup, N. C. Maynard, J. A. Schoendorf, K. D. Siebert, D. R. Weimer, W. W. White, and G. R. Wilson (2002), Hill model of transpolar potential saturation: Comparisons with MHD simulations, *J. Geophys. Res.*, *107*(A6), 1075, doi:10.1029/2001JA000109.

Skoug, R. M., J. T. Gosling, J. T. Steinberg, D. J. McComas, C. W. Smith, N. F. Ness, Q. Hu, and L. F. Burlaga (2004), Extremely high speed solar wind: 29–30 October 2003, *J. Geophys. Res.*, *109*, A09102, doi:10.1029/2004JA010494.

St.-Maurice, J. P., W. Kofman, and E. Kluzek (1990), Electron heating by plasma waves in the high latitude E region and related effects: Observations, *Adv. Space Res.*, *10*(6), 225–237.

Y. S. Dimant, C. Goodrich, and V. G. Merkin, Center for Space Physics, Boston University, 725 Commonwealth Ave., Boston, MA 02215, USA. (vgm@bu.edu)

J. Lyon, Department of Physics and Astronomy, Dartmouth College, Hanover, NH 03755, USA.

G. Milikh, K. Papadopoulos, and A. S. Sharma, Department of Astronomy, University of Maryland, College Park, College Park, MD 20742, USA.

M. Wiltberger, High Altitude Observatory, National Center for Atmospheric Research, Boulder, CO 80301, USA.